

Magnetism | Hot Paper |

Structural and Magnetic Variations in a Family of Isoskeletal, Oximate-Bridged $\{\text{Mn}^{\text{IV}}_2\text{M}^{\text{III}}\}$ Complexes ($\text{M}^{\text{III}} = \text{Mn, Gd, Dy}$)Alysha A. Alaimo,^[a] Anne Worrell,^[a] Sayak Das Gupta,^[b] Khalil A. Abboud,^[b] Christos Lampropoulos,^[c] George Christou,^[b] and Theocharis C. Stamatatos*^[a]

Abstract: The self-assembly reaction of $\text{MnCl}_2 \cdot 4\text{H}_2\text{O}$, acenaphthenequinone dioxime (acndH_2) and NEt_3 has yielded an unprecedented, linear $\{\text{Mn}^{\text{IV}}_2\text{M}^{\text{III}}\}$ complex with an $S = 5$ spin ground state and non-SMM behavior. The targeted replacement of the central Mn^{III} ion with Gd^{III} and Dy^{III} ions has successfully increased the S and turned on the SMM dynamics without affecting the core structure and the nature of the magnetic exchange interactions.

High-spin molecules and single-molecule magnets (SMMs) are two of the most attractive areas of research within the field of molecular magnetism.^[1] This is mainly due to the applications that these molecular species could potentially find in spintronics, information storage, quantum computation, as well as multiferroic materials and magnetic refrigerants.^[2] High-spin molecules containing an appreciable number of unpaired electrons in their spin ground state, S , predominantly result from ferromagnetic exchange interactions between the paramagnetic metal ions. Such type of interactions is rare, especially in polynuclear compounds, due to the unpredictability of the ligands' behavior and their interactions with metal orbitals. When the ground state is combined with a large and negative zero-field splitting parameter, D , these coordination compounds could exhibit magnetic bistability and superparamagnetic-like properties attributed to an overall SMM behavior.^[3] Therefore, SMMs show frequency-dependent, out-of-phase, χ''_{M} , ac signals and magnetic hysteresis below a blocking temperature. This is due to the slow relaxation of magnetization over (thermally assisted) and/or through (quantum tunneling of magnetization) an anisotropic energy barrier, U_{eff} , that separates opposite orientations of the $\pm ms$ states.^[4]

For more than two decades, 1st-row transition-metal ions have been key elements for the preparation of aesthetically beautiful complexes, high-spin molecules and SMMs.^[5] Specifically, it was shown that Jahn–Teller (JT) distorted, high-spin and anisotropic, Mn^{III} ions can self-assemble into polymetallic cluster compounds exhibiting diverse nuclearities and SMM properties, with large U_{eff} values and high blocking temperatures.^[1] That has been indeed the case for the ubiquitous families of Mn_{12} -carboxylate ($U_{\text{eff}} = 74 \text{ K}$)^[4] and Mn_6 -oximate ($U_{\text{eff}} = 86 \text{ K}$) SMMs,^[6] and more recently for a nano-sized $\{\text{Mn}_3\}$ complex with U_{eff} of 60 K .^[7] In all cases, though, there has been limited predictability on the resulting magnetic properties, because it is extremely difficult, if not impossible, to simultaneously control both the spin ground state and the magnetic anisotropy of these complex systems.^[8]

For many years, the general belief has been that a very large spin ground state would be vital for the enhancement of SMM dynamics, which however, is not always the case. Powell and co-workers reported a $\{\text{Mn}_{19}\}$ cluster compound with a record spin of $S = 83/2$; however, this complex showed no SMM behavior.^[9] During almost the same period, lanthanide (Ln) complexes started to evolve as superior candidates for enhanced SMM properties.^[10] This was in part due to their large single-ion anisotropies, resulting from the unquenched spin-orbit coupling. For these homometallic $4f$ -based complexes, it was proven that an easy-axis magnetic anisotropy is favored when the ligand field stabilizes the state with the largest projection of the total angular momentum.^[11] These results have prompted scientists to prepare heterometallic $3d/4f$ -clusters, and especially $\text{Mn}^{\text{III}}/\text{Ln}$ ones, as means of combining large S values with significant magnetic anisotropies, thus achieving a level of control towards the SMM properties.^[12] To this end, the aforementioned $\{\text{Mn}_{19}\}$ cluster has been successfully transformed to a $\{\text{DyMn}_{18}\}$ SMM via the deliberate replacement of an 8-coordinate Mn^{II} ion with Dy^{III} .^[13] The only other example – to our knowledge – where a homometallic Mn-containing non-SMM was converted to a Mn/Ln SMM is that of the antiferromagnetic $\{\text{Mn}^{\text{II}}_2\text{Mn}^{\text{III}}_4\}$ to $\{\text{Dy}_2\text{Mn}^{\text{III}}_4\}$.^[14]

We herein report (i) the self-assembly synthesis of a rare, ferromagnetically coupled but non-SMM $\{\text{Mn}^{\text{III}}\text{Mn}^{\text{IV}}_2\}$ (1) complex, bearing exclusively the dianion of the acenaphthenequinone dioxime (acndH_2 , Figure 1, bottom) bridging/chelating ligand [IUPAC name: *N,N'*-dihydroxy-1,2-acenaphthylenediimine], and (ii) its deliberate conversion to both a larger-spin $\{\text{GdMn}^{\text{IV}}_2\}$ (2) compound and a $\{\text{DyMn}^{\text{IV}}_2\}$ (3) SMM, without affecting the nuclearity, topology, metal oxidation state descriptions, and the

[a] A. A. Alaimo, A. Worrell, Dr. T. C. Stamatatos
Department of Chemistry, Brock University
1812 Sir Isaac Brock Way, L2S 3A1 St. Catharines, Ontario (Canada)
E-mail: tstatamatatos@brocku.ca

[b] S. D. Gupta, K. A. Abboud, Prof. Dr. G. Christou
Department of Chemistry, University of Florida
Gainesville, Florida 32611-7200 (USA)

[c] Dr. C. Lampropoulos
Department of Chemistry, University of North Florida
1 UNF Dr., Jacksonville, Florida 32224 (USA)

Supporting information and the ORCID number(s) for the author(s) of this article can be found under <https://doi.org/10.1002/chem.201706098>.

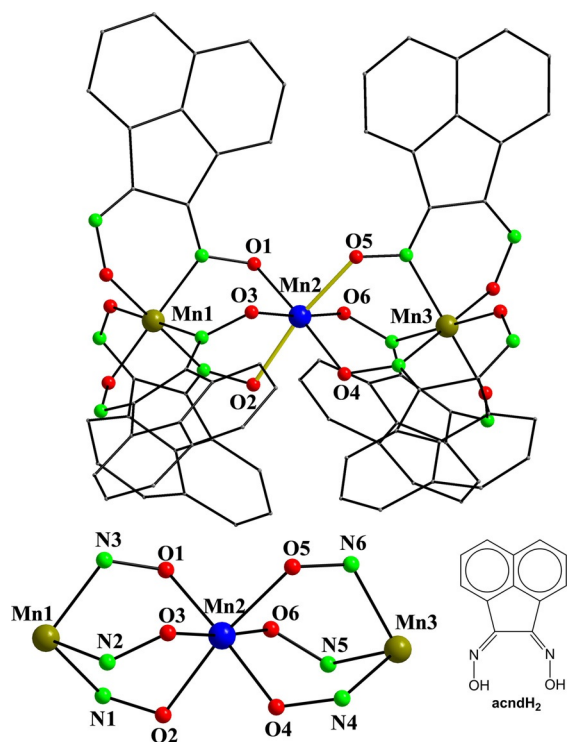


Figure 1. Partially labeled representations of the anion of **1** (top) and its $[\text{Mn}_3(\mu\text{-NO})_6]^{5+}$ core (bottom). The structure of the ligand acndH_2 is also shown. The Jahn–Teller axial elongations of the central Mn^{III} ion are highlighted with yellow thick bonds. H atoms have been omitted for clarity. Color Scheme: Mn^{III} blue, Mn^{IV} olive green, N green, O red, C gray.

nature of predominant magnetic exchange interactions. The oximate-bridged complexes **1–3** manifest themselves as a rare opportunity for a comprehensive magneto-structural correlation investigating in depth the $\text{Mn}\cdots\text{Mn}$ and $\text{Mn}\cdots\text{Ln}$ magnetic coupling, since they are nearly isoskeletal and perhaps most importantly, they are oxido-free bridged.^[15]

The one-pot reaction of $\text{MnCl}_2\cdot 4\text{H}_2\text{O}$, acndH_2 , and NEt_3 in a 1:2:2 molar ratio in a solvent mixture comprising MeOH/DMF led to a dark brown solution, which was allowed to evaporate slowly at room temperature. After 3 days, dark-brown plate-like crystals of complex $(\text{NHEt}_3)[\text{Mn}^{\text{III}}\text{Mn}^{\text{IV}}_2(\text{acnd})_6(\text{MeOH})_2]\cdot 2\text{L}\cdot\text{MeOH}$ (**1**) were obtained in 55% yield. The oxidation states of the Mn ions and the formula of **1** were confirmed by inspection of the metric parameters, charge balance considerations, and bond valence sum (BVS) calculations.^[16] As a result, the central Mn ion ($\text{Mn}2$) was assigned to the 3+ oxidation state while the two extrinsic Mn ions ($\text{Mn}1$ and $\text{Mn}3$) were 4+. All the $\text{Mn}\text{--}\text{O}$ and $\text{Mn}\text{--}\text{N}$ bond distances fall into the expected range for similar compounds of high-spin Mn^{III} and Mn^{IV} ions with O- and N-donor atoms.^[6,15] The “open”-like structure of the anion of **1** (Figure 1, top) can be described as an almost linear array of three Mn ions ($\text{Mn}1\text{--}\text{Mn}2\text{--}\text{Mn}3$ angle = 174.8°) linked to each other through the oximate arms of six doubly deprotonated acnd^{2-} ligands. The central Mn^{III} ion is octahedrally coordinated to six oximate O atoms, whereas the two external, distorted octahedral Mn^{IV} ions are capped by the “chelating” NO-part of three acnd^{2-} ligands; the latter are thus acting in an $\eta^1\text{:}\eta^1\text{:}\eta^1\text{:}\mu$ fash-

ion. Two axial elongations of the $\text{Mn}2\text{--}\text{O}2$ (2.096(6) Å) and $\text{Mn}2\text{--}\text{O}5$ (2.090(6) Å) distances confirmed the presence of the expected, for a d^4 ion, JT distortion. The six $\text{Mn}^{\text{IV}}\text{--}\text{N}\text{--}\text{O}\text{--}\text{Mn}^{\text{III}}$ torsion angles within the $[\text{Mn}_3(\mu\text{-NO})_6]^{5+}$ core (Figure 1, bottom) are significantly twisted and they span the range $46.1\text{--}53.2^\circ$. All individual torsion angles are larger than the cutoff torsion angle of $\approx 31^\circ$,^[15] which infers predominant ferromagnetic exchange interactions between the Mn ions (vide infra). The intramolecular $\text{Mn}^{\text{III}}\cdots\text{Mn}^{\text{IV}}$ and $\text{Mn}^{\text{IV}}\cdots\text{Mn}^{\text{IV}}$ separations are 3.534(2)/3.518(2) Å and 7.045(2) Å, respectively. The acenaphthene moieties of the acnd^{2-} ligands are also involved into intermolecular $\pi\text{--}\pi$ stacking interactions, which result in the formation of pseudo-1D chains of weakly interacting $\{\text{Mn}_3\}$ clusters (Figure S1). The shortest $\text{Mn}\cdots\text{Mn}$ separation between neighboring $\{\text{Mn}_3\}$ clusters in the crystal is 10.13(2) Å.

It is interesting to note that according to the HSAB principle it would be expected the harder, oximate O atoms to opt for coordination to the Mn^{IV} rather than the Mn^{III} ions. Even though this was not the case in **1**, this is not totally surprising as oximate $\text{C}=\text{N}\text{--}\text{O}^-$ groups are strong α -nucleophiles and very often their N atoms can satisfy the coordination needs of both soft and hard acids.^[17] In addition, it is very likely that the six-membered chelate rings around the external metal ions are more stable for the smaller in size Mn^{IV} , rather than the larger Mn^{III} . This, in combination with the pronounced oxophilicity of 4f-metal ions, prompted us to target the replacement of the central Mn^{III} with Gd^{III} and Dy^{III} ions. To this end, the same reaction that led to **1** was repeated in the presence of excess $\text{Gd}(\text{acac})_3\cdot\text{H}_2\text{O}$ or $\text{Dy}(\text{acac})_3\cdot\text{H}_2\text{O}$ salts ($\text{acac}^- = \text{acetylacetonate}$). Under the same crystallization conditions, dark-brown crystals of complexes $(\text{NHEt}_3)[\text{Gd}^{\text{III}}\text{Mn}^{\text{IV}}_2(\text{acnd})_6(\text{MeOH})_2]\cdot 2\text{L}\cdot\text{MeOH}$ (**2**) and $(\text{NHEt}_3)[\text{Dy}^{\text{III}}\text{Mn}^{\text{IV}}_2(\text{acnd})_6(\text{MeOH})_2]\cdot 2\text{L}\cdot 0.5\text{MeOH}$ (**3**) were obtained over a period of two weeks in yields of 50 and 40%, respectively. BVS calculations confirmed the Mn^{IV} oxidation state descriptions for **2** and **3**.^[16] The neutral acenaphthene ketone-mono-oxime groups (L), found in the crystal lattice of both **2** and **3**, were most likely derived from the in situ metal-assisted hydrolysis of the parent acndH_2 ligand. These L groups are intramolecularly H-bonded to the coordinated MeOH molecules.

The structures of the isoskeletal, heterometallic complexes **2** (Figure S2) and **3** (Figure 2) are very similar to each other and, although reminiscent to the overall core topology of **1** (Figure S3), there are some striking differences that merit further discussion. Firstly, the structures of **2** and **3** are more “bent” than linear; the $\text{Mn}1\text{--}\text{Gd}1\text{--}\text{Mn}2$ and $\text{Mn}1\text{--}\text{Dy}1\text{--}\text{Mn}2$ angles are 143.6 and 143.0° , respectively. The intramolecular $\text{Mn}^{\text{IV}}\cdots\text{Ln}^{\text{III}}$ and $\text{Mn}^{\text{IV}}\cdots\text{Mn}^{\text{IV}}$ separations are in the range 4.006(1)–4.033(2) Å and 7.603(2)/7.653(3) Å, respectively, larger than the corresponding distances found in **1**. The $\text{Mn}^{\text{IV}}\text{--}\text{N}\text{--}\text{O}\text{--}\text{Ln}^{\text{III}}$ torsion angles in **2** and **3** are again very twisted and they range between 42.7° and 62.3° . Furthermore, both Gd^{III} and Dy^{III} ions are 8-coordinate, bearing two additional MeOH groups in their coordination spheres. The coordination geometry of both 4f-metal ions is distorted triangular dodecahedral, as determined by the program SHAPE (CSHM values of 0.23 (Gd) and 0.19 (Dy); Figure S4 and Table S4).^[18] Finally, complexes **1–3** are all unique in their metal core topologies, nuclearities and oxida-

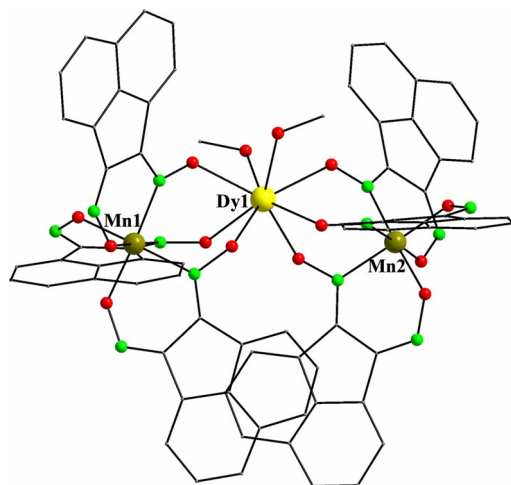


Figure 2. Structure of the anion of **3**. Color Scheme: Dy^{III} yellow, Mn^{IV} olive green, N green, O red, C gray.

tion state descriptions.^[19] This inspired us to undertake a detailed study of their bulk magnetic properties and magnetization dynamics.

Variable-temperature direct-current (*dc*) magnetic susceptibility measurements were performed on freshly prepared and analytically pure microcrystalline samples of **1–3** in the temperature range 5–300 K in an applied field of 0.1 T. The data are shown as $\chi_M T$ versus *T* plots in Figure 3. The values of the $\chi_M T$ products for all three compounds at 300 K are higher than the values of 6.75, 11.63, and 17.92 cm³·mol⁻¹·K, expected for Mn^{III}/2Mn^{IV}, Gd^{III}/2Mn^{IV}, and Dy^{III}/2Mn^{IV} non-interacting ions, respectively. The $\chi_M T$ of **1** steadily increases with decreasing *T*, reaching a maximum of 12.73 cm³·mol⁻¹·K at 26 K, and then slightly decreases to 9.86 cm³·mol⁻¹·K at 5 K. The low-*T* decrease is likely due to Zeeman effects from the applied *dc* field, weak intermolecular antiferromagnetic interactions, low-lying excited states, and/or zero-field splitting (ZFS). For both complexes **2** and **3**, the $\chi_M T$ product remains essentially constant in the 30–300 K temperature range, indicating the presence of weak ex-

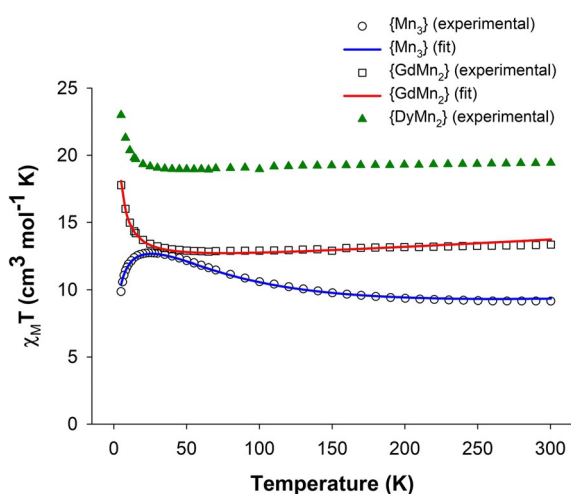


Figure 3. $\chi_M T$ versus *T* plots for **1–3** in a 1 kG field. The solid lines are the fits of the data; see the text for the fit parameters.

change interactions between the metal centres, and then it increases to 17.78 and 23.00 cm³·mol⁻¹·K at 5 K, respectively. The shapes of the curves for the oximate-bridged **1–3** clearly suggest the presence of predominant ferromagnetic exchange interactions between the metal ions, and consequently the stabilization of large spin ground states.

This was confirmed for **1** and **2** by fitting the experimental $\chi_M T$ versus *T* data to an isotropic 2-*J* model that includes both Mn^{IV}...M^{III} (M^{III} = Mn or Gd; as *J*₁) and Mn^{IV}...Mn^{IV} (as *J*₂) interactions. Good fits of the data (blue and red solid lines in Figure 3) in the entire temperature range 300–5 K were obtained using the program PHI ($H = -2J_{ij}\hat{S}_i\hat{S}_j$ convention).^[20] The best-fit parameters were: *J*₁ = +10.9(1) cm⁻¹, *J*₂ = -0.3(1) cm⁻¹, *g* = 1.98(2) for **1**, and *J*₁ = +0.15(2) cm⁻¹, *J*₂ ≈ 0 cm⁻¹, *g* = 2.01(2) for **2**, thus establishing the ferromagnetic interactions between the Mn^{IV}...M^{III} pairs and the weak to negligible interactions between the next-nearest Mn^{IV}...Mn^{IV} pairs. These findings agree with the type of interactions expected for Mn-containing pairs that are bridged by significantly “twisted” oximate groups.^[6,15] As a result, complexes **1** and **2** possess the maximum possible *S* = 5 and 13/2 ground states, respectively. For the isotropic {GdMn^{IV}₂} system, the *S* = 13/2 ground state was additionally confirmed by magnetization (*M*) versus field (*H*) studies at 2 K, and the extrapolation of $\chi'_M T$ *ac* data down to 0 K. In this regard, the magnetization of **2** appears to saturate fast to a value of ≈ 13 *N*_B at relatively low fields (Figure S5), and the $\chi'_M T$ product is heading to a value of ≈ 24.5 cm³·mol⁻¹·K (Figure S6), both in agreement with an *S* = 13/2 ground state. The $\chi'_M T$ value expected for an *S* = 13/2 spin state is 24.38 cm³·mol⁻¹·K (calculated for *g* = 2).

Ac magnetic susceptibility studies were also performed for the potentially anisotropic **1** and **3** to assess their magnetization dynamics in the absence of an external *dc* field. The {Mn^{III}Mn^{IV}₂} complex **1** does not show any out-of-phase signals but the {Dy^{III}Mn^{IV}₂} analogue exhibits frequency-dependent tails of χ''_M *ac* signals below 6 K (Figure 4), consistent with the superparamagnetic slow relaxation of an SMM. The presence of the anisotropic Dy^{III} ion has apparently contributed to the onset of slow magnetization relaxation. The absence of well-resolved peaks in the χ''_M versus *T* diagram of **3** is indicative of a fast-relaxing SMM with a relatively small energy barrier.^[3,11] The latter was approximated by using the equation:^[21] $\ln(\chi''/\chi') = \ln(\omega\tau_0) + E_a/k_B T$. Considering a single relaxation process, the least-square-fits of the experimental data (inset of Figure 4) gave an average energy barrier of ≈ 5.8(1) K and a τ_0 of 2(1) × 10⁻⁶ s. The application of a small external *dc* field of 0.1 T has not resulted in an appreciable change of the magnetization dynamics (Figure S7). The energy barrier was again approximated by using the aforementioned equation (Figure S8). The fit of the data gave: *E*_a = 6.7(2) K and a τ_0 of 3(2) × 10⁻⁶ s.

In summary, we have shown that it is indeed feasible to both adjust, or tweak, the spin of an already high-spin molecule,^[22] and turn on the SMM properties by altering the central, trivalent metal ion in a family of isoskeletal {Mn^{IV}M^{III}Mn^{IV}}–oximate complexes. This is done in a way that does not alter the core structure and the nature of predominant magnetic interactions. Furthermore, this constitutes proof-of-feasibility for

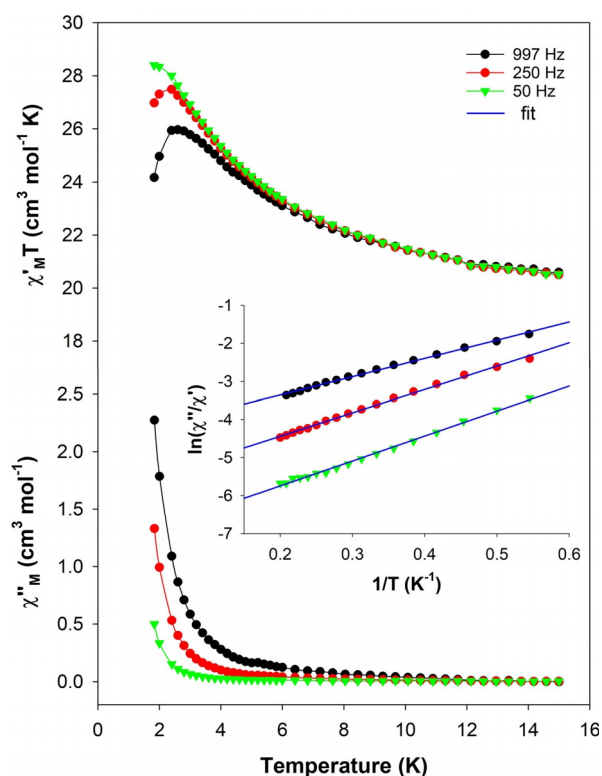


Figure 4. Temperature dependence of the in-phase (as $\chi'_{M,T}$, top) and out-of-phase (χ''_{M} , bottom) *ac* magnetic susceptibilities for **3**, measured in a 3.5 G *ac* field oscillating at the indicated frequencies, in the absence of an external *dc* field. (inset) Plots of $\ln(\chi''_{M}/\chi')$ versus $1/T$ for **3**; the blue solid lines are the best-fit curves.

spin- and SMM-switching in other Mn^{III} -containing high-spin and non-SMM complexes by deliberate replacement of some or all Mn^{III} by 4*f*-metal ions. In this case, the spin was tweaked by 13%, from $S=5$ in $\{\text{Mn}^{\text{III}}\text{Mn}^{\text{IV}}_2\}$ to $S=6.5$ in the $\{\text{Gd}^{\text{III}}\text{Mn}^{\text{IV}}_2\}$ analogue. In addition, we are currently trying to synthesize and characterize new $\{\text{Ln}^{\text{III}}\text{Mn}^{\text{IV}}_2\}$ members of this family of trinuclear compounds with either different ligand fields around the Ln^{III} ion or different *f*-orbital electron densities (i.e., oblate and prolate) as a means of enhancing the overall anisotropy of the systems and consequently the SMM dynamics. This targeted approach to high-spin molecules and SMMs could be further developed and expanded to a plethora of other Mn and Mn–Ln cluster compounds primarily bridged by oximate-based ligands. With this work we are adding an important new tool to the arsenal of coordination chemists toward the development of molecule-based magnetic materials.

Experimental Section

All manipulations were performed under aerobic conditions using chemicals and solvents as received. The acndH_2 and the lanthanide(III) acetylacetonate precursors, $\text{Ln}(\text{acac})_3\cdot\text{H}_2\text{O}$ ($\text{Ln}=\text{Gd}, \text{Dy}$), were synthesized as previously reported.^[23]

Synthesis of 1

To a stirred, yellow solution of acndH_2 (0.04 g, 0.2 mmol) and NEt_3 (28 μL , 0.2 mmol) in MeOH/DMF (15 mL, 1:2 v/v) was added solid $\text{MnCl}_2\cdot 4\text{H}_2\text{O}$ (0.02 g, 0.1 mmol). The resulting orange-red suspension was stirred for 2 h, during which time all the solids dissolved, and the color of the solution changed to dark brown. The resulting solution was left to evaporate slowly at room temperature, and within 3 days dark brown plate-like crystals of complex **1**· H_2O formed. The crystals were collected by filtration, washed with cold MeOH (2×2 mL) and dried in air. The yield was 55%. Selected IR data (ATR): 3129 (w), 1585 (m), 1500 (wb), 1420 (m), 1291 (m), 1238 (w), 1165 (m), 1128 (m), 1067 (s), 1021 (s), 996 (s), 953 (m), 898 (vs.), 822 (s), 768 (vs.), 737 (m), 707 (m), 600 (vs.), 549 (m), 518 (m), 462 (m), 439 (m); elemental analysis (%) calcd for **1** ($M_w=1528.18 \text{ g mol}^{-1}$): C 61.31, H 3.43, N 11.92; found: C 61.19, H 3.22, N 12.05.

Synthesis of 2 and 3

To a stirred, yellow solution of acndH_2 (0.04 g, 0.2 mmol) and NEt_3 (28 μL , 0.2 mmol) in MeOH/DMF (15 mL, 1:2 v/v) were added together solids $\text{MnCl}_2\cdot 4\text{H}_2\text{O}$ (0.02 g, 0.1 mmol) and $\text{Gd}(\text{acac})_3\cdot\text{H}_2\text{O}$ (0.15 g, 0.3 mmol) or $\text{Dy}(\text{acac})_3\cdot\text{H}_2\text{O}$ (0.15 g, 0.3 mmol). The resulting red suspensions were stirred for 2 h, during which time all the solids dissolved, and the color of the solutions changed to dark brown. The resulting solutions were diffused with hexanes (15 mL), and within 2 weeks dark brown plate-like crystals of complexes **2**·2L-MeOH and **3**·2L·0.5MeOH formed. The crystals were collected by filtration, washed with cold MeOH (2×2 mL) and dried in air. The yields were 50 and 40%, respectively. The IR spectra of **2** and **3** are almost identical to each other. Selected IR data (ATR) for representative **2**: 3130 (w), 1718 (m), 1586 (w), 1510 (w), 1483 (w), 1419 (m), 1292 (m), 1275 (m), 1214 (m), 1173 (m), 1130 (m), 1095 (m), 1075 (m), 1021 (m), 996 (m), 959 (m), 900 (s), 863 (m), 823 (s), 771 (vs.), 727 (w), 671 (w), 597 (m), 490 (mb), 440 (m). Elemental analysis (%) calcd for **2**·2 L ($M_w=2088.97 \text{ g mol}^{-1}$): C 59.80, H 3.57, N 10.06; found: C 59.93, H 3.74, N 9.95; elemental analysis (%) calcd for **3**·2 L ($M_w=2094.22 \text{ g mol}^{-1}$): C 59.65, H 3.56, N 10.03; found: C 59.87, H 3.73, N 9.93.

Acknowledgements

This work was supported by the NSERC-DG, ERA and Brock University (to Th.C.S), the Research Corp. (to C.L), and the National Science Foundation (grants CHE-1565664 to G.C, and DMR-1429428/ DMR-1626332 to C.L).

Conflict of interest

The authors declare no conflict of interest.

Keywords: cluster compounds · high-spin molecules · manganese · oxime ligands · single-molecule magnets

[1] C. Papatriantafyllopoulou, E. E. Moushi, G. Christou, A. J. Tasiopoulos, *Chem. Soc. Rev.* **2016**, *45*, 1597.

[2] a) L. Ouahab, "Multifunctional Molecular Materials", Pan Stanford Publishing Pte. Ltd. **2013**; b) R. Vincent, S. Klyatskaya, M. Ruben, W. Wernsdorfer, F. Balestro, *Nature* **2012**, *488*, 357; c) M. Urdampilleta, S. Klyatskaya, J.-P. Cleuziou, M. Ruben, W. Wernsdorfer, *Nat. Mater.* **2011**, *10*,

- 502; d) M. Evangelisti, F. Luis, L. J. de Jongh, M. Affronte, *J. Mater. Chem.* **2006**, *16*, 2534.
- [3] R. Sessoli, D. Gatteschi, J. Villain, *Molecular Nanomagnets*, Oxford University Press, Oxford, UK, **2006**.
- [4] R. Bagai, G. Christou, *Chem. Soc. Rev.* **2009**, *38*, 1011.
- [5] a) C. J. Milios, R. E. P. Winpenny, *Struct. Bonding (Berlin)* **2015**, *164*, 1; b) G. A. Craig, M. Murrie, *Chem. Soc. Rev.* **2015**, *44*, 2135.
- [6] C. J. Milios, A. Vinslava, W. Wernsdorfer, S. Moggach, S. Parsons, S. P. Perlepes, G. Christou, E. K. Brechin, *J. Am. Chem. Soc.* **2007**, *129*, 2754.
- [7] P. Abbasi, K. Quinn, D. I. Alexandropoulos, M. Damjanović, W. Wernsdorfer, A. Escuer, J. Mayans, M. Pilkington, Th. C. Stamatatos, *J. Am. Chem. Soc.* **2017**, *139*, 15644.
- [8] a) F. Neese, D. Pantazis, *Faraday Discuss.* **2011**, *148*, 229; b) O. Waldmann, *Inorg. Chem.* **2007**, *46*, 10035.
- [9] A. M. Ako, I. J. Hewitt, V. Mereacre, R. Clérac, W. Wernsdorfer, C. E. Anson, A. K. Powell, *Angew. Chem. Int. Ed.* **2006**, *45*, 4926; *Angew. Chem.* **2006**, *118*, 5048.
- [10] N. Ishikawa, M. Sugita, T. Ishikawa, S. Koshihara, Y. Kaizu, *J. Am. Chem. Soc.* **2003**, *125*, 8694.
- [11] a) J. D. Rinehart, J. R. Long, *Chem. Sci.* **2011**, *2*, 2078; b) R. Layfield, M. Murugesu, *Lanthanides and Actinides in Molecular Magnetism*, Wiley, **2015**; c) J. Tang, P. Zhang, *Lanthanide Single Molecule Magnets*, Springer, **2015**.
- [12] a) H. L. C. Feltham, S. Brooker, *Coord. Chem. Rev.* **2014**, *276*, 1; b) H. Ke, L. Zhao, Y. Guo, J. Tang, *Dalton Trans.* **2012**, *41*, 2314; c) X.-L. Li, F.-Y. Min, C. Wang, S.-Y. Lin, Z. Liu, J. Tang, *Dalton Trans.* **2015**, *44*, 3430.
- [13] A. M. Ako, V. Mereacre, R. Clérac, W. Wernsdorfer, I. J. Hewitt, C. E. Anson, A. K. Powell, *Chem. Commun.* **2009**, 544.
- [14] M. Savva, K. Skordi, A. D. Fournet, A. E. Thuijs, G. Christou, S. P. Perlepes, C. Papatriantafyllopoulou, A. J. Tasiopoulos, *Inorg. Chem.* **2017**, *56*, 5657.
- [15] R. Inglis, L. F. Jones, C. J. Milios, S. Datta, A. Collins, S. Parsons, W. Wernsdorfer, S. Hill, S. P. Perlepes, S. Piligkos, E. K. Brechin, *Dalton Trans.* **2009**, 3403.
- [16] See the Supporting Information.
- [17] C. J. Milios, Th. C. Stamatatos, S. P. Perlepes, *Polyhedron* **2006**, *25*, 134.
- [18] M. Llunell, D. Casanova, J. Girera, P. Alemany, S. Alvarez, *SHAPE*, version 2.0, Barcelona, Spain, **2010**.
- [19] a) C.-L. Zhou, Z.-M. Wang, B.-W. Wang, S. Gao, *Dalton Trans.* **2012**, *41*, 13620; b) T. Pathmalingham, S. I. Gorelsky, T. J. Burchell, A.-C. Bédard, A. M. Beauchemin, R. Clérac, M. Murugesu, *Chem. Commun.* **2008**, 2782; c) F. Habib, G. Brunet, F. Loiseau, T. Pathmalingham, T. J. Burchell, A. M. Beauchemin, W. Wernsdorfer, R. Clérac, M. Murugesu, *Inorg. Chem.* **2013**, *52*, 1296; d) F. Birkelbach, U. Flörke, H.-J. Haupt, C. Butzlaff, A. X. Trautwein, K. Wiegardt, P. Chaudhuri, *Inorg. Chem.* **1998**, *37*, 2000; e) C. Lampropoulos, Th. C. Stamatatos, K. A. Abboud, G. Christou, *Inorg. Chem.* **2009**, *48*, 429.
- [20] N. F. Chilton, R. P. Anderson, L. D. Turner, A. Soncini, K. S. Murray, *J. Comput. Chem.* **2013**, *34*, 1164.
- [21] J. Bartolomé, G. Filoti, V. Kuncser, G. Schinteie, V. Mereacre, C. E. Anson, A. K. Powell, D. Prodius, C. Turta, *Phys. Rev. B* **2009**, *80*, 014430.
- [22] Th. C. Stamatatos, K. A. Abboud, W. Wernsdorfer, G. Christou, *Angew. Chem. Int. Ed.* **2007**, *46*, 884; *Angew. Chem.* **2007**, *119*, 902.
- [23] a) P. Richardson, K. J. Gagnon, S. J. Teat, G. Lorusso, M. Evangelisti, J. Tang, Th. C. Stamatatos, *Cryst. Growth Des.* **2017**, *17*, 2486; b) M. F. Richardson, W. F. Wagner, D. E. Sands, *Inorg. Chem.* **1968**, *7*, 2495.

Manuscript received: December 22, 2017

Accepted manuscript online: January 9, 2018

Version of record online: January 25, 2018